ISSN 0036-0295, Russian Metallurgy (Metally), Vol. 2018, No. 12, pp. 1101–1107. © Pleiades Publishing, Ltd., 2018.
Original Russian Text © N.V. Petrushin, E.G. Arginbaeva, E.S. Elyutin, I.A. Treninkov, 2018, published in Elektrometallurgiya, 2018, No. 5, pp. 7–16.

MANUFACTURE OF FERROUS AND NONFERROUS METALS

Structural and Phase Characteristics of the Ni_3Al-Based Intermetallic Alloy Fabricated by High-Gradient Directional Solidification and Selective Laser Melting

N. V. Petrushin[a], *, E. G. Arginbaeva[a], E. S. Elyutin[a], and I. A. Treninkov[a]

[a] *Federal State Unitary Enterprise All-Russia Scientific Research Institute of Aviation Materials, State Research Center of the Russian Federation, Moscow, Russia*

**e-mail: nv_petrushin@mail.ru*

Received December 19, 2017

Abstract—The microstructure and the phase composition of an experimental Ni_3Al-based intermetallic alloy containing (wt %) 7.8 Al, 14.5 Ta, 0.9 Mo, 0.5 W, 0.5 Re, 0.15 C, and Ni for balance, which was prepared by slow (6 mm/h) high-gradient (15°C/mm) directional solidification and selective laser melting, are studied, and the lattice parameters of phases and solidus and liquidus temperatures are determined. The phase compositions of the intermetallic alloy samples prepared by these technologies are found to be identical and consist of a γ′-phase matrix and TaC carbide particles.

Keywords: high-gradient directional solidification, selective laser melting, intermetallic alloys, Ni_3Al (γ′ phase), lattice parameter, solidus and liquidus temperatures

DOI: 10.1134/S0036029518120121

INTRODUCTION

Owing to a number of unique properties, Ni_3Al (γ′ phase)-based intermetallic alloys are among the advanced structural materials intended for manufacturing he cast parts of aviation gas turbine engines operating at temperatures up to 1200–1250°C for a long time. The most known compositions are casting heat-resistant (γ′ + γ) alloys of the VKNA (VIN) series [1, 2]. These alloys are used to manufacture turbine blades with single-crystal and polycrystalline structures by directional and equiaxial solidification, respectively. The single crystals and polycrystals of high-temperature nickel and (γ′ + γ) alloys that are produced under nonequilibrium directional and equiaxial solidification conditions in accordance with available industrial manufacturing processes [3] have dendritic cellular structure and are characterized by substantial chemical, structural, and phase inhomogeneity due to dendrite microsegregation of alloying components during solidification [4, 5].

The slow directional solidification of multicomponent alloys at a high temperature gradient in a melt occurs in the absence of microsegregation of alloying elements along the direction parallel to the solidification front surface and allows one to form castings structurally homogeneous over the section. However, in this case, microsegregation of alloying elements at the solidification front takes place and, as a result, a casting, which is characterized by a variable composition and physicochemical properties along the part length, forms [6].

The use of selective laser melting (SLM) of powder multicomponent compositions allows one to decrease the segregation inhomogeneity of the material of parts substantially. SLM is assumed to show promise as a manufacturing process for the parts of aviation and other industries [7–11]. As regards to the high-temperature structural materials prepared by SLM, the majority of works are related to heat-resistant nickel alloys exhibiting a high weldability [12–14]. However, the use of SLM for manufacturing materials by melting of powder compositions of casting heat-resistant nickel alloys and intermetallics is of particular interest [15].

The aim of the present study is to study the structural and phase characteristics of an experimental Ni_3Al-based intermetallic alloy prepared by two manufacturing processes, namely, by slow high-gradient solidification and SLM of a powder alloy composition.

EXPERIMENTAL

We studied an experimental intermetallic alloy, the composition of which comprises (wt %) 7.8 Al, 14.5 Ta, 0.9 Mo, 0.5 W, 0.5 Re, 0.15 C, and Ni for balance. The

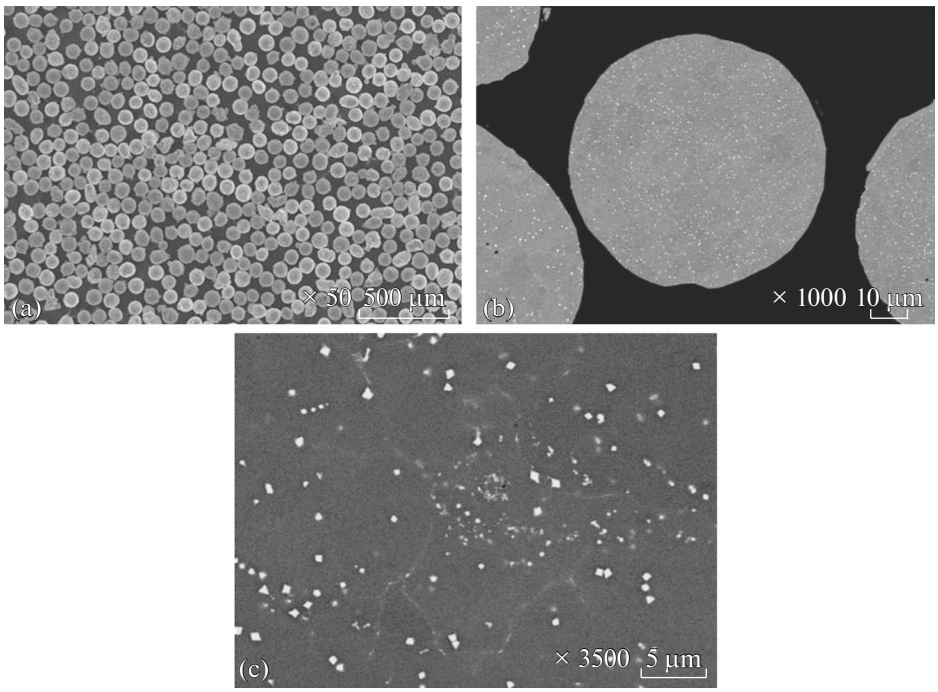

Fig. 1. (a) Appearance and (b, c) microstructure of intermetallic alloy granules prepared by inert gas sputtering; white particles are TaC carbide.

Al and Ta concentrations in the alloy were selected so that they corresponded to the composition of the intermetallic γ′-phase in the isothermal section of the Ni–Al–Ta phase diagram at 1000°C [17].

A primary intermetallic alloy ingot was melted in a vacuum induction furnace. According to differential thermal analysis (DTA) data, the temperature range of melting of the primary alloy is 1263–1357°C. DTA was performed using an HDSC PT 1750 installation. Chemical analysis of the alloy was performed on a Varian 730-ES atomic emission spectrometer and CS-600 and TC-600 gas analyzers. According to the experimental data, the composition of the melted primary intermetallic alloy is close to the selected calculated composition; the contents of sulfur, oxygen, and nitrogen impurities are 0.002, 0.001, and 0.001%, respectively.

The directional solidification of the intermetallic alloy was carried out by the Bridgman method [6] at an axial temperature gradient in a melt of 15°C/mm and a growth rate of 6 mm/h. A blank for the directional solidification was cut from the intermetallic alloy ingot and placed in a corundum crucible (~15 mm in inner diameter and ~100 mm in length) mounted on the crystallizer rod in the thermal unit of the laboratory directional solidification installation.

The casting (~15 mm in diameter and ~90 mm in length) prepared by directional solidification was used to cut (along the casting) a plate-shaped blank ~5 mm thick. Samples for the DTA determination of the solidus and liquidus temperatures were cut from different areas of the plate. The remaining part of the casting was cut in disks ~8 mm long; each of the disks was used to prepare cross and longitudinal microsections for the investigation of the structural and phase characteristics of the alloy by scanning electron microscopy and electron microprobe and X-ray diffraction (XRD) analyses. Each of the disk-shaped samples corresponded to one or another volume fraction q of the directionally solidified alloy.

To perform SLM synthesis of samples, the melt of the cast primary intermetallic alloy was sputtered by an argon flow (gas atomization method) using a HERMIGA10/100VI [18] installation, and the alloy-composition powder with a particle size of 63–80 μm was prepared. Figure 1 shows the microstructure of intermetallic alloy granules. Some granules have a cellular structure with a cell size of ~10 μm; fine tantalum carbide particles (~0.2 μm in size) are distributed within the cells and at their boundaries.

SLM of the intermetallic alloy powder was performed in a high-purity argon atmosphere using an EOS M 290 installation [15]. The layer-by-layer synthesis of samples (~15 mm in diameter and ~70 mm in length) was performed in accordance with the conditions developed in the All-Russia Institute of Aviation Materials. Melting of the powder material during synthesis was performed in accordance with the preset algorithm of hatching in the form of a track having a substantial curvature of cross-section profile at the side of preceding melted layer.

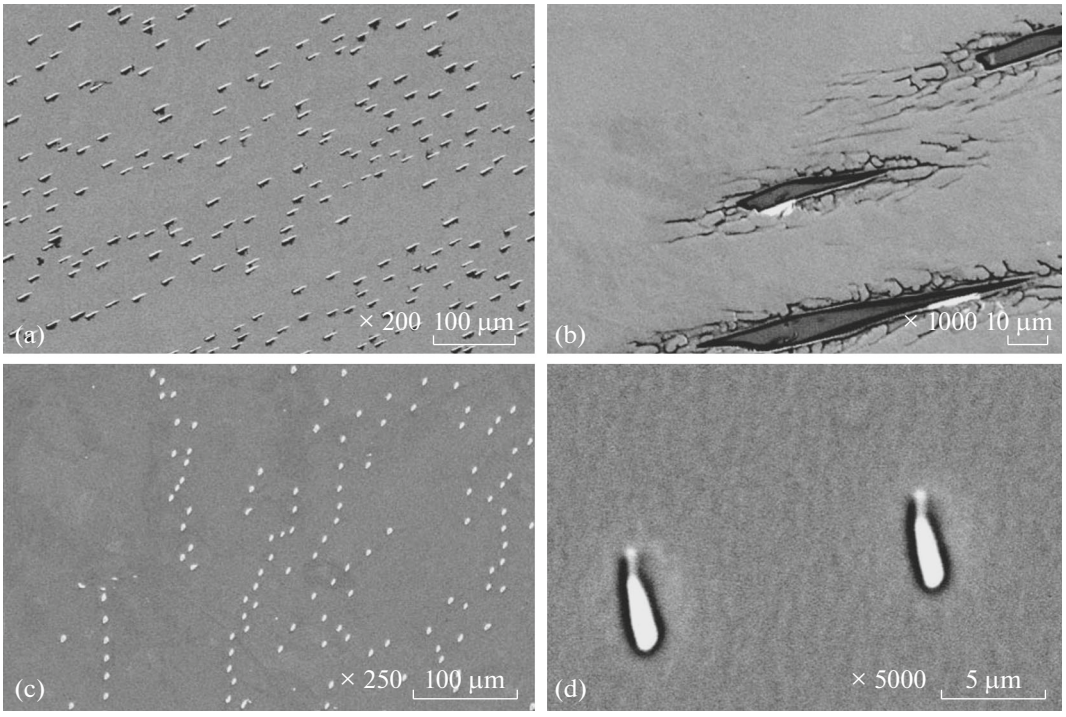

Fig. 2. Microstructure of intermetallic alloy in the oriented growth zone of casting subjected to slow (6 mm/h) directional solidification at a high temperature gradient (15°C/mm): (a, b) longitudinal and (c, d) cross sections.

The microstructure and chemical compositions of the alloy and phases were studied on a JSM-6490 LV and a ZeissEVOMA 10 scanning electron microscopes. XRD analysis was performed using an Empyrean diffractometer, Cu$K\alpha$ radiation, and Bragg–Brentano focusing geometry.[1] X-ray diffraction patterns were processed and the lattice parameters were determined using the Highscore+ special-purpose software.

RESULTS AND DISCUSSION

Structural and Phase Characteristics of the Intermetallic Alloy Prepared by Directional Solidification

As a result of slow directional solidification at a high temperature gradient at the growth front, a unidirectional structure forms in the casting, which consists of columnar γ'-phase intermetallic grains with the $\langle 001 \rangle$ crystallographic orientation. Grains are arranged along the longitudinal axis of casting; the axial misorientation is up to 30°. Plate-like precipitates are observed within columnar grains and at their boundaries; the precipitates were identified as the TaC carbide (Fig. 2). The matrix surrounding the carbide precipitates is heterophase and consists of rounded γ'-phase particles separated by thin nickel γ solid solution layers (see Fig. 2b). The cross-section of the casting demonstrates a cellular structure.

According to the chemical analysis data (averaged over the cross section) for the disk samples cut from the casting, the aluminum, tantalum, and molybdenum contents in the γ' phase slightly decrease when the fraction of solid q increases (Table 1). Therefore, these elements are rejected to the solid during solidification; i.e., the distribution coefficients of these elements are more than unity. The other alloying elements (W, Re) weakly segregate during the directional solidification of the intermetallic alloy; in average, their concentrations are unchanged along the casting length. The tantalum content in the carbide phase decreases slightly and the molybdenum and nickel contents increase; no tungsten and rhenium were found in the carbide. The distribution of the alloying elements in the γ' and TaC phases over the section of intermetallic alloy casting was found to be unchanged. In accordance with the slight changes in the alloy composition along the casting length and the absence of segregation of alloying elements across the casting section, the solidus and liquidus temperatures of the intermetallic alloy casting determined by DTA are $T_S = 1384$ and $T_L = 1424$°C, respectively. These temperatures exceed those ($T_S = 1263$ and $T_L = 1357$°C) for the alloy prepared by equiaxial solidification.

During XRD analysis of the intermetallic alloy prepared by slow directional solidification (6 mm/h) at the high temperature gradient (15°C/mm), the (003)

[1] A.N. Raevskikh took part in this part of the work.

Table 1. Chemical composition of phases in different sections of intermetallic alloy casting (for different fractions q of solid)

Volume fraction of solid phase q, %	Phase	Element content, wt %					
		Al	Ta	Ni	Mo	W	Re
9*	γ′	7.7	13.6	76.4	1.1	0.8	0.5
	Carbide MC	–	84.7	0.6	2.2	–	–
56*	γ′	7.5	13.4	76.5	0.9	1.0	0.7
	Carbide MC	–	81.0	1.3	4.0	–	–
100**	γ′	7.3	10.9	79.6	0.8	0.9	0.5
	γ	5.2	3.7	87.9	2.6	0.2	0.5
	Carbide MC	–	78.9	6.7	2.8	–	–

* Oriented growth zone.
** End of casting.

Table 2. Structural and phase characteristics of the γ′ phase of the intermetallic alloy prepared by different methods

Preparation method	Phase	Lattice parameter, nm	FWHM, deg	Deviation of longitudinal axis from the ⟨001⟩ columnar-grain orientation, deg
Directional solidification at the fraction of solid phase:				
$q = 9\%$	γ'_1	0.35891	0.152	20.4
	γ'_2	0.36047	0.250	
$q = 80\%$	γ'_1	0.35805	0.276	29.6
	γ'_2	0.35831	0.136	
	γ'_3	0.35870	0.155	
	γ'_4	0.35987	0.272	
SLM	γ′	0.35803	0.7431	–

and (004) reflections were analyzed (Fig. 3). The (003) reflection is a superlattice reflection; therefore, it is forbidden for the γ-phase crystal lattice. The amount of the γ′ reflections and their arrangement in the (004) doublet were determined using the (003) reflection. The γ phase was not found in all samples cut in the casting zone with the oriented growth structure. In one of the samples (q = 9%), the γ′ phase (γ'_1 fraction) of a certain composition dominates, whereas the γ′ phase, which has another composition (γ'_2 fraction) and substantially higher both lattice parameter and full width at half maximum (FWHD), is present in the form of traces (Table 2, Fig. 3b). In another sample (q = 80%), four compositions (fractions) of the γ′ phase were detected, which differ in the structural characteristics (see Table 2). It should be noted that the increase in the FWHM for the γ'_2 (q = 9%) fraction and γ'_1, γ'_2, γ'_3, and γ'_4 (q = 80%) intermetallic phase in the alloy is substantial as compared to that for the γ'_1 fraction (q = 9%); in total case, one of the causes for the fact is the high inhomogeneity of their chemical composition.

Structural and Phase Characteristics of the Intermetallic Alloy Prepared by Selective Laser Melting

The studies of the intermetallic alloy prepared by SLM showed that, during synthesis and subsequent cooling, subgrains are formed within tracks, which differ from one another in orientation and size (Figs. 4a, 4b). The subgrains consist of columnar crystals and, in cross section, have a shape of cells (see Figs. 4c, 4d). Micropores up to 10 μm in diameter are found within the subgrains (see Fig. 4e). The structure of the subgrains in the intermetallic alloy is close to that of the other casting heat-resistant nickel alloys

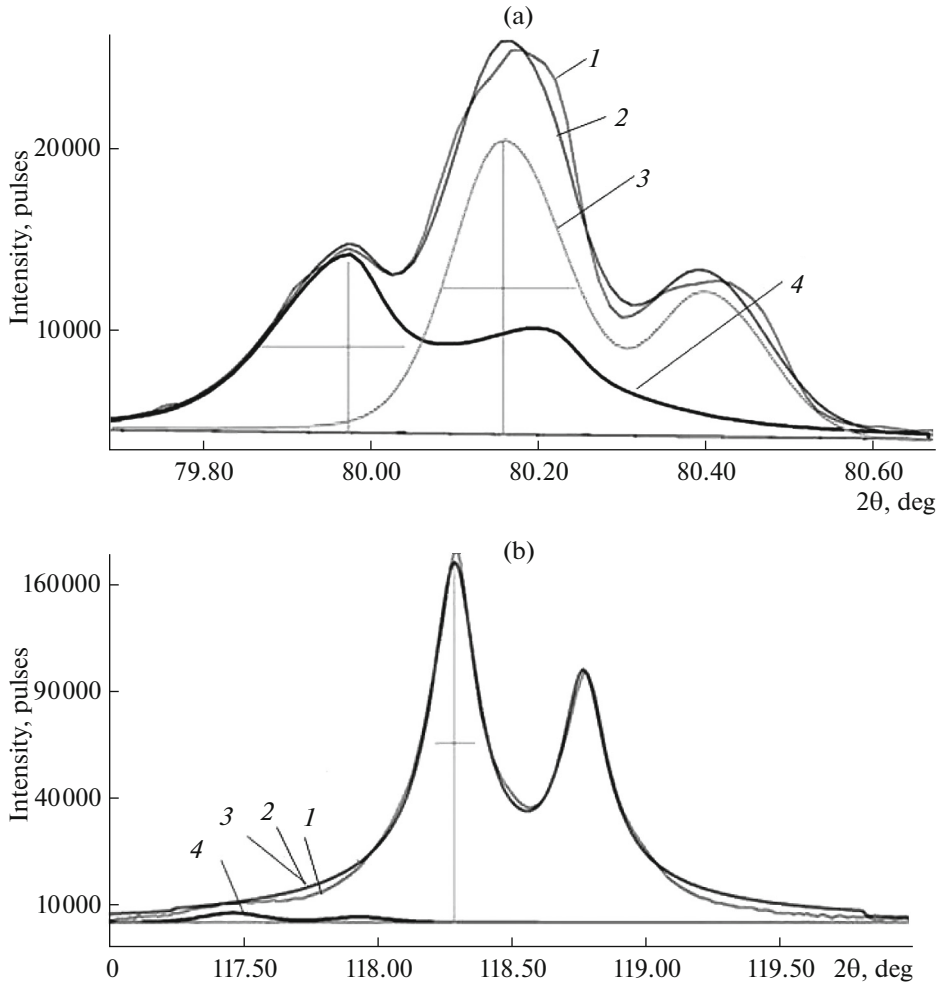

Fig. 3. Portions of the X-ray diffraction patterns with (a) γ′ (003) superlattice and (b) γ′ (004) fundamental reflections taken with Cu$K\alpha$ radiation and the resolution of the experimental γ′-phase reflections into phase singlets of the γ'_1 and γ'_2 phases of the intermetallic alloy subjected to slow directional solidification at a rate of 6 mm/h and a high temperature gradient of 15°C/mm (casting section q = 9%): (*1*) experimental reflection, (*2*) approximation of experimental reflection, (*3*) first singlet profile (γ'_1), and (*4*) second singlet profile (γ'_2). The intensity scale is linear and quadratic root for the (003) and (004) reflections, respectively.

prepared by SLM [15, 19] and consists of cut first-order dendrites. The average dendrite cell diameter is ~1 μm. Fine disperse precipitates (<0.1 μm) are located at cell boundaries; according to XRD data, the precipitates are tantalum carbides (Fig. 5). Because of high internal stresses within tracks, microcracks up to 300 μm in length are formed at cell boundaries (Fig. 4b). The microcracks are arranged mainly in the building plane; this is likely to be related to the generation of internal stresses during SLM and the shape of formed tracks [15].

According to XRD data, the synthesized intermetallic alloy and the alloy prepared by slow directional solidification at a high temperature gradient have similar phase compositions. The XRD pattern (Fig. 5) shows that the SLM alloy consists of two phases: Ni_3Al-based γ′ phase (lattice parameter is 0.35803 nm) and TaC carbide (fcc lattice and a lattice parameters of 0.44130 nm). The absence of fundamental reflections corresponding to the nickel γ solid solution indicates that the formation of the γ phase in the structure of the synthesized intermetallic alloy is suppressed even at the ultrahigh solidification rate typical of SLM (~10^6°C/s [20]).

According to DTA data, the solidus and liquidus temperatures of the synthesized intermetallic alloy are 1379 and 1412°C, respectively. These temperature are approximately equal to those of the alloy prepared by slow directional solidification at a high temperature gradient (1384 and 1424°C, respectively).

The obtained results show that the principal structural and phase characteristics of the intermetallic alloy prepared by SLM almost coincide with those of the alloy subjected to slow high-gradient directional solidification. The FWHM of the γ′-phase reflection for the alloy prepared by SLM is an exception (see

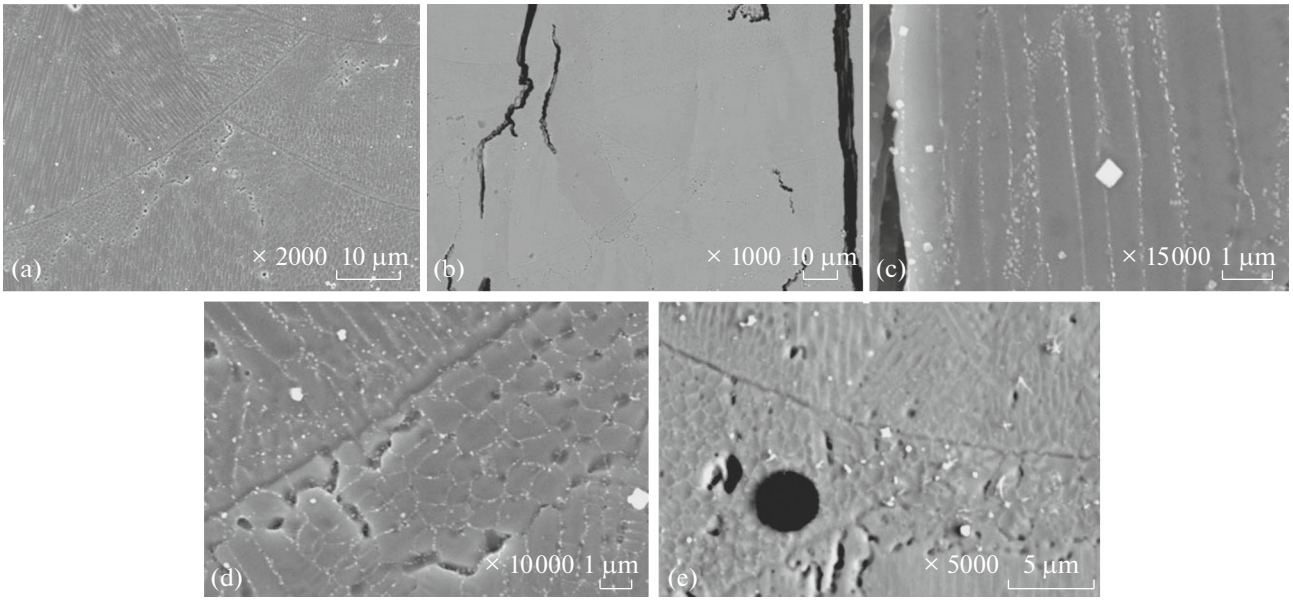

Fig. 4. Microstructure of intermetallic alloy prepared by SLM: (a) subgrains with different cell orientations within tracks, (b) microcracks at subgrain boundaries, (c) γ′-phase cells and fine TaC carbide particles at cell boundaries, and (d) micropore within γ′-phase cell.

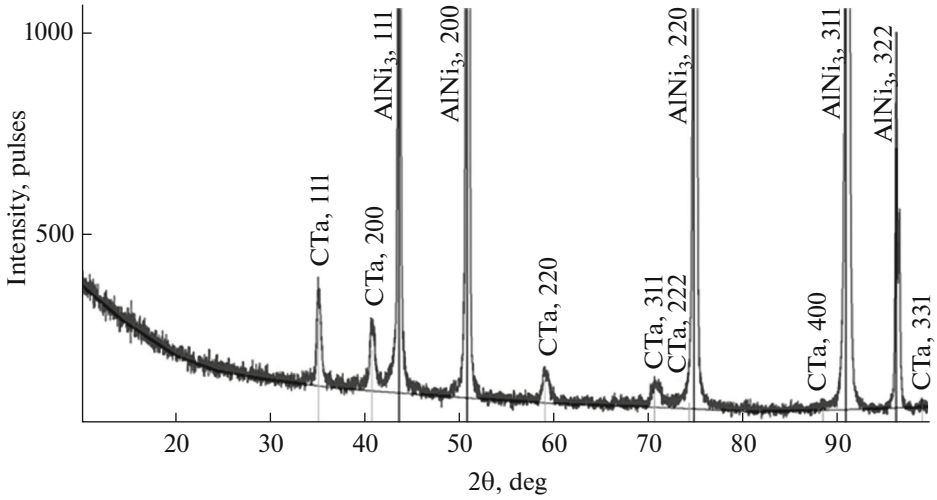

Fig. 5. X-ray diffraction pattern of the intermetallic alloy prepared by SLM.

Table 2). The FWHM of the alloy is several times higher than that for the γ′ phase of the alloy prepared by high-gradient directional solidification. This is likely to indirectly confirm the existence of high stresses in γ′-phase subgrains of the alloy prepared by SLM.

CONCLUSIONS

(1) During slow (6 mm/h) directional solidification at a high temperature gradient (15°C/mm) of an experimental Ni_3Al-based intermetallic alloy containing (wt %) 7.8 Al, 14.5 Ta, 0.9 Mo, 0.5 W, 0.5 Re, 0.15 C, and Ni for balance, the casting consisting of columnar γ′-phase grains with the ⟨001⟩ crystallographic orientation forms. Within the columnar grains and at their boundaries, platelike TaC precipitates are observed.

(2) It was found that, during slow directional solidification at a high temperature gradient, the aluminum, tantalum, and molybdenum concentrations in the γ′ phase along the casting decrease slightly; their distribution coefficients is more than unity. During directional solidification of the alloy, weakly segregation of tungsten and rhenium takes place. Neither tungsten nor rhenium is found in the TaC-based carbide. In accordance with the slight change of the alloy composition along the casting length, the solidus and

liquidus temperatures remain unchanged, 1384 and 1424°C, respectively.

(3) It was found that the γ′ phase in the intermetallic alloy subjected to directional solidification consists of several fractions differing in the crystal lattice parameter (0.35805–0.36047 nm) and FWHM for the γ′-phase reflection (0.136°–0.276°).

(4) An intermetallic alloy was synthesized by selective laser melting.

(5) It was found that the track structure of the synthesized intermetallic alloy containing (wt %) 7.8 Al, 14.5 Ta, 0.9 Mo, 0.5 W, 0.5 Re, 0.15 C, and Ni balance consists of columnar γ′ cells up to 1 μm in lateral size, which are oriented within a subgrain. Subgrain boundaries are decorated with fine (<0.1 μm) TaC-based carbide particles. Microcracks form at the boundaries.

(6) The lattice parameters of the γ′ phase (0.35803 nm) and TaC carbide (0.44130 nm) were determined and the solidus (1379°C) and liquidus (1412°C) temperatures of the synthesized intermetallic alloy were measured. The FWHM of the γ′-phase reflection is 0.743°.

ACKNOWLEDGMENTS

This study was performed in terms of scientific direction 2.1. Fundamental Investigations (Strategic Directions for Developing Materials and Technologies up to 2030) [16]. This study was supported by the Foundation of President of the Russian Federation for supporting the leading scientific schools (project no. NSh9831.2016.8).

REFERENCES

1. E. N. Kablov, O. G. Ospennikova, and O. A. Bazyleva, "Materials for highly thermal-loaded gas turbine engines," Vestn. Bauman MGTU, Ser. Mashinostroenie, No. SP2, 13–19 (2011).
2. E. N. Kablov, O. G. Ospennikova, and N. V. Petrushin, "New single-crystal γ′-phase-based alloy for gas turbine blades," Aviatsionnye Mater. Tekhnologii, No. 1 (34), 34–40 (2015). doi 10.18577/2071-9140-2015-0-1-34-40
3. V. V. Gerasimov, E. M. Vasik, V. A. Nikitin, and M. G. Zernova, "Experience in exploiting the casting technology of VKNA-4U alloy blade sectors with the single-crystal structure," Aviatsionnye Mater. Tekhnologii, No. 4, 13–18 (2012).
4. A. A. Drozdov, K. B. Povarova, A. E. Morozov, A. V. Antonova, M. A. Bulakhtina, and N. A. Alad'ev, "Dendrite segregation in Ni_3Al-based intermetallic single crystals alloyed with Cr, Mo, W, Ti, Co, and Re", Russ. Metall., No. 7, 551–557 (2015).
5. M. R. Orlov, N. V. Petrushin, A. G. Evgenov, and F. N. Karachevtsev, "Homogenization processes in single-crystal and granulated heat-resistant ZhS32 alloy," Elektrometallurgiya, No. 1, 15–26 (2017).
6. N. V. Petrushin and E. V. Monastyrskaya, "Application of directional solidification to solve problems of the development and optimization of heat-resistant materials," Materialovedenie, No. 5, 2–10 (1998).
7. I. Yadroitsev and I. Smurov, "Selective laser technology: from the single laser melted track stability to 3D parts of complex shape," Physics Procedia **5**, 551–560 (2010).
8. T. L. Trineva, "Manufacturing process of casting rigging from a composite material by selective laser sintering," Protsessy Lit'ya, No. 1 (19), 31–35 (2012).
9. M. A. Zlenko, A. A. Popovich, and I. N. Mutylina, *Additive Technologies in Mechanical Engineering* (Izd. Politekhnicheskogo Univ., Saint Petersburg, 2013).
10. E. N. Kablov, "Trends and Guidelines of Innovative Development of Russia," in *Collective Book of Scientific and Information Materials*, 3rd ed. (VIAM, Moscow, 2015).
11. V. G. Smelov, A. V. Sotov, and A. V. Agapovichev, "Research on the possibility of restoring blades while repairing gas turbine engines parts by selective laser melting," IOP Conf. Ser: Mater. Sci. Eng. **140** (1), 012019 (2016). doi 10.1088/1757-899X/140/1/012019
12. V. Sh. Sufiyarov, A. A. Popovich, E. V. Borisov, and I. A. Polozov, "Selective laser melting of heat-resistant nickel alloy," Tsvetn. Met., No. 1 (865), 79–84 (2015).
13. J. Strößner, M. Terock, and U. Glatzel, "Mechanical and structural investigation of nickel-based superalloy IN718 manufactured by selective laser melting (SLM)," Adv. Eng. Mater. **17** (8), 1099–1105 (2015).
14. A. G. Evgenov, M. A. Gorbovets, and S. M. Prager, "Structure and mechanical properties of VZh159 and EP648 heat-resistant alloys prepared by selective laser melting," Aviatsionnye Mater. Tekhnologii, No. S1 (43), 8–15 (2016).
15. A. G. Evgenov, E. A. Lukina, and V. A. Korolev, "Peculiarities of selective laser synthesis process with regard to casting nickel- and intermetallic Ni_3Al-based alloys," Novosti Materialoved. Nauka Tekhnika, No. 5 (23), 3–11 (2016).
16. E. N. Kablov, "Innovative developments of FSUE "VIAM" SSC of RF on realization of Strategic directions in developing materials and their processing technologies up to 2030," Aviatsionnye Mater. Tekhnologii, No. 1 (34), 3–33 (2015). doi 10.18577/2071-9140-2015-0-1-3-33
17. P. Nash and D. R. F. West, "Phase equilibria in the Ni–Ta–Al system," Met. Sci. **13** (12), 670–676 (1979).
18. A. G. Evgenov, S. V. Nerush, and S. A. Vasilenko, "Manufacturing and testing of fine disperse metallic powder of high-chromium nickel-based alloy for laser LMD buildup," Trudy VIAM, No. 5, 04, (2014). http://www.via-works.ru. Cited October 7, 2016. doi 10.18577/2307-6046-2014-0-5-4-4
19. A. V. Zavodov, N. V. Petrushin, and D. V. Zaitsev, "Microstructure and phase composition of ZhS32 heat-resistant alloy after selective laser melting, vacuum heat treatment, and hot isostatic pressing," Pis'ma Materialakh **7** (2), 111–116 (2017). http://www.letersonmaterials.com. doi 10.22226/2410-3535-2017-2-111-116
20. L. Yali and G. Dongdong, "Parametric analysis of thermal behavior during selective laser smelting additive manufacturing of aluminum alloy powder," Mater. Design **63**, 856–867 (2014).

Translated by N. Kolchugina